MDPI

Article

Comparison between three paradigms of General Relativity

Kareema Al Hosni [1,†,‡] and Mudhahir Al Ajmi [2,*]

[1] Sultan Qaboos University; kareema.alhosni@gmail.com
[2] Sultan Qaboos University; mudhahir@squ.edu.om
* Correspondence: kareema.alhosni@gmail.com
‡ These authors contributed equally to this work.

Abstract: Gravity formulated as a classical gauge theory is based on the Mach principle in terms of curvature scalar R by A. Einstein. The original idea of Einstein limits the gravity to act as a curvature in spacetime. However, there exist other possible classical fields such as torsion and non-metricity. The aim of this paper is to make a compatible comparison between three paradigms: Gravity as curvature via Einstein-Hilbert action, Teleparallel Gravity (TEGR) and Coincidence Gravity (CGR). In TEGR a flat spacetime is considered as well as an asymmetric connection metric. In CGR, gravity is constructed in an equally flat tortionless spacetime which is ascribed to non-metricity. The strength and weakness of each formulation is tested in the framework of a homogeneous and isotropic cosmological background. Mainly, the equivalence between GR and TEGR is examined at the level of equation of motion. Also, we study the interactions between dark energy, dark matter and radiation and the stability of these models is explored. The implications of the interaction were tested in both early and late epoch of the Universe. It has been found that mostly there is a similarity of description of the evolution of the Universe provided by GR and TEGR while CGR always showed different description.

Keywords: Torsion; non-metricity.

Citation: Al Hosni, K.; Al Ajmi, M. Title. *Universe* **2021**, *1*, 0. https://dx.doi.org/10.3390/universe1010000

Received:
Accepted:
Published:

1. Introduction

Modifications of general relativity (GR) was motivated by the discovery of the accelerated expansion of the Universe. Therefore, a number of theories have been established based on particular approaches [1]. GR describes the geometric properties of spacetime, taking the curvature as a fundamental geometrical object. The best-known representation of GR at which gravity is formulated with the dynamic of curvature in spacetime by the Hilbert action

$$\mathcal{S} = \frac{1}{2\kappa^2}\int d^4x\sqrt{-g}R + \mathcal{S}_m. \tag{1}$$

Here $\mathcal{S}_m$ is the mater action which is defined as $\mathcal{S}_m = \int \mathcal{L}_m\sqrt{-g}d^4x$ and $\kappa^2 = 8\pi G$ and it is called the gravitational coupling.[2]
Although GR is a very elegant theory that succeed to describe many phenomena, it still suffers from flaws that invoke the demand for finding alternative description for gravity. One of the problems that GR faces is the cosmological constant problem. Einstein equations bring out the scenario of the dark energy by setting the cosmological constant. The cosmological constant is the simplest interpretation for dark energy that represents a constant energy density of empty space. Nevertheless, there is an incompatibility in the theoretical and observational calculation of the cosmological constant. The cosmological constant problem has serious impacts in the description of the evolution of the Universe.
Other equivalent geometrical descriptions of gravity, are the Teleparallel Gravity and Coincedince General Relativity. The former is based on torsion and the later is based on non-metricity.

- **Teleparallel Equivalence of General Relativity**

Teleparallel Gravity is based on torsion and vanishing curvature. It is mapped in non-Riemmanian geometry called Wietznbock [7]. Tetrads basis vector e^i_μ is the essential quantity in Teleparallel gravity. They are defined by [3]

$$g_{\mu\nu} = e^i_\mu e^j_\nu \eta_{ij} \tag{2}$$

where η_{ij} is flat Minkowski metric. Teleparallel is extended to what is called $f(\mathcal{T})$ gravity, where $f(\mathcal{T})$ indicates an arbitrary function for torsion, such that, it reduces to TEGR if $f(\mathcal{T}) = \mathcal{T}$ [4]. General action for $f(\mathcal{T})$ gravity reads

$$S = \frac{1}{2\kappa^2}\int d^4x e(\mathcal{T} + f(\mathcal{T})) + S_m. \tag{3}$$

Here S_m is the action of matter, and $\mathcal{T}$ is

$$\mathcal{T} = S^{\mu\nu}_\sigma \mathcal{T}^\sigma_{\mu\nu}, \tag{4}$$

where

$$S^{\mu\nu}_\sigma = \frac{1}{2}(K^{\mu\nu}_\sigma + \delta^\mu_\sigma \mathcal{T}^{\rho\nu}_\rho - \delta^\mu_\sigma \mathcal{T}^{\rho\mu}_\rho)$$
$$K^{\mu\nu}_\sigma = -\frac{1}{2}(\mathcal{T}^{\mu\nu}_\sigma - \mathcal{T}^{\nu\mu}_\sigma - \mathcal{T}^{\mu\nu}_\sigma).$$

- **Coincidence General Relativity**

Further modification was made by formulating GR via the non-metricity. The non-metricity is the fundamental object in Coincedence General Relativity which is the derivative of the metric tensor. It is attributed to flat and torsion-free spacetime which implies that vectors stay parallel along the space [5]. In Coincidence GR (CGR), the inertial effect vanishes which means that the connection $\Gamma^\sigma_{\mu\nu} = 0$, [1] and this gives CGR an advantage over GR. Another advantage for CGR is that it can be achieved without the need of boundary terms [2]. The general action for a non-metricity scalar is :

$$\mathcal{S} = \int d^4x\sqrt{-g}\mathcal{Q} + S_m. \tag{5}$$

Evidences show that we now live at a special cosmic epoch; which is a transition from decelerating to accelerating Universe and from matter-dominated to Universe dark-energy-dominated Universe [6]. The reason for this is that the volume of space increases as the Universe expands, so the density of matter decreases. On the other hand, the density of dark energy does not change as the Universe expands. Hence, the density of dark energy is higher than that of matter in the current time. There are several models that can be presumed for dark energy. For instance, cosmological constant, quintessence and phantom energy.

In order to describe the phenomenon of dark energy, numerous models has been introduced which are based on the interaction of dark energy with dark matter or any other types of fluid. As established in GR, the cosmological constant is a simple solution to dark energy. Quintessence and phantom energy are alternative models to describe the dark energy which represent components that have negative pressure. They are dynamical quantities that can be characterized by their equation of state [9]. Most of models which represent quintessence have $w < -\frac{1}{3}$, phantom energy $w < -1$ and cosmological constant has $w = -1$ [10]. The larger the value of w, the smaller its accelerating. The cosmological constant does not evolve with time, whereas the quintessential does [9].

In this paper we are interested in comparing the evolution of the Universe described by the three theories (GR, TEGR and CGR). The paper is organized as follows: In

section 2 the equations and mathematical models used in the project are introduced. Sections 3 represents the cosmological models and stability analysis of GR, TEGR and CGR respectively along with the results for each paradigm. In the last section 4, the numerical solutions plots that describe the evolution of the Universe are shown.

2. Materials and Methods

We investigate the cosmological dynamics for the three theories; GR, TEGR and CGR. Considering Friedmann-Lemaitre-Roberson-Walker (FLRW) metric:

$$g_{\mu\nu} = diag(1, -a(t)^2, -a(t)^2, -a(t)^2), \tag{6}$$

where $a(t)$ is the scale factor, the Friedmann equations take a general form as

$$\begin{aligned} 3H &= \kappa^2 \sum \rho_i, \\ 2\dot{H} &= -\kappa^2 \sum (P_i + \rho_i). \end{aligned} \tag{7}$$

Here H is the Hubble, where $H = \frac{\dot{a}(t)}{a(t)}$. Also, P_i is pressure and ρ_i is the density. The pressure and density are represented here generally. However, they are considered to represent the pressure and density mainly for three types of fluids which are dark energy, dark matter and radiation respectively;

$$\begin{aligned} P_i &= P_\Lambda + P_m + P_r + ... \\ \rho_i &= \rho_\Lambda + \rho_m + \rho_r + ... \end{aligned} \tag{8}$$

Because these fluids are taken to be perfect fluids we can write $P = w\rho$, where w is the equation of state parameter. For dark matter $w_m = 0$, for radiation $w_r = \frac{1}{3}$ and w_λ is for dark energy. The corresponding continuity equations for the three fluids:

$$\begin{aligned} \dot{\rho}_\Lambda + 3H(\rho_\Lambda + P_\Lambda) &= \beta_\Lambda, \\ \dot{\rho}_m + 3H(\rho_m + P_m) &= \beta_m \\ \dot{\rho}_r + 3H(\rho_r + P_r) &= \beta_r, \end{aligned} \tag{9}$$

where β is the interaction parameter which describe how the considered fluids interact with each other such that $\beta_\Lambda + \beta_m + \beta_r = 0$. For this work we constructed two models of interaction:

- Model-I of interaction

$$\beta_\Lambda = \alpha_\Lambda \frac{H^3}{\kappa^2} \Omega_\Lambda \Omega_m \tag{10}$$

$$\beta_m = \alpha_m \frac{H^3}{\kappa^2} \Omega_r \Omega_m \tag{11}$$

$$\beta_r = \alpha_r \frac{H^3}{\kappa^2} \Omega_m (\Omega_\Lambda - \Omega_r), \tag{12}$$

- Model-II of interaction

$$\beta_\Lambda = \alpha_\Lambda \frac{H^3}{\kappa^2} \Omega_r (\Omega_\Lambda - \Omega_m) \tag{13}$$

$$\beta_m = \alpha_m \frac{H^3}{\kappa^2} \Omega_m (\Omega_\Lambda - \Omega_r) \tag{14}$$

$$\beta_r = \alpha_r \frac{H^3}{\kappa^2} \Omega_\Lambda (\Omega_m - \Omega_r). \tag{15}$$

The stability of the corresponding dynamical systems will be analyzed around the critical points. The dynamical system is ascribed to a dimensionless density parameter Ω, which is defined as:

$$\Omega = \frac{\rho}{\rho_c}.$$

Here ρ_c is the critical density. Henceforth, we have:

$$\rho_\Lambda = \frac{3H^2}{\kappa^2}\Omega_\Lambda,\ \rho_m = \frac{3H^2}{\kappa^2}\Omega_m,\ \rho_r = \frac{3H^2}{\kappa^2}\Omega_r. \tag{16}$$

Here Ω_Λ, Ω_m and Ω_r are density parameter corresponding to dark energy, dark matter and radiation respectively, whereas α_Λ, α_m and α_r are coupling constants. To construct a dynamical system of Ω instead of ρ, we use the e-folding parameter $N = \ln(a) = -\ln(1+z)$, so that the derivative density parameter will be taken with respect to N, $(\frac{d\Omega}{dN})$. The Jacobi stability of dynamical systems will be applied. To apply the Jacobi stability consider

$$\frac{d\Omega}{dN} = f(\Omega). \tag{17}$$

The function f is called vector field. A point Ω is a *fixed point* or *critical point* for which $f(\Omega) = 0$. The linearization is implemented by Hartman theorem which states that the differential system and the linearized system are topologically equivalent, if they are treated locally [11]. To linearize the vector field around this point, we define the Jacobian matrix J such that [7]

$$J = (Df)|_p = \frac{\partial f_i}{\partial \Omega_i}|_p \tag{18}$$

and specifically for our study, we have

$$\begin{bmatrix} \frac{\partial f_1}{\partial \Omega_\Lambda} & \frac{\partial f_1}{\partial \Omega_m} & \frac{\partial f_1}{\partial \Omega_r} \\ \frac{\partial f_2}{\partial \Omega_\Lambda} & \frac{\partial f_2}{\partial \Omega_m} & \frac{\partial f_2}{\partial \Omega_r} \\ \frac{\partial f_3}{\partial \Omega_\Lambda} & \frac{\partial f_3}{\partial \Omega_m} & \frac{\partial f_3}{\partial \Omega_r} \end{bmatrix}$$

where

$\mathrm{f}_1 = \frac{d\Omega_\Lambda}{dN}$, $f_2 = \frac{d\Omega_m}{dN}$ and $f_3 = \frac{d\Omega_r}{dN}$.

3. Numerical Solutions

3.1. General Relativity

3.1.1. Dynamical Systems and Stability analysis

Consider equations 7, the pressure and the density are

$$\begin{aligned} \rho_i &= \rho_\Lambda + \rho_m + \rho_r \\ P_i &= P_\Lambda + P_m + P_r \end{aligned} \tag{19}$$

We constructed the system of equations of the density parameter according to the two models of interaction and find the corresponding fixed points. We have:

- Model I of interaction

Now, we write the dynamical system of density parameter corresponding the Model-I of interaction as

$$\frac{d\Omega_\Lambda}{dN} = 3\Omega_\Lambda[(1+w_\Lambda)\Omega_\Lambda + \Omega_m + \frac{4}{3}\Omega_r] - 3(1+w_\Lambda)\Omega_\Lambda + \frac{\alpha_\Lambda \Omega_\Lambda \Omega_m}{3} \quad (20)$$

$$\frac{d\Omega_m}{dN} = 3\Omega_m[(1+w_\Lambda)\Omega_\Lambda + \Omega_m + \frac{4}{3}\Omega_r] - 3\Omega_m + \frac{\alpha_m \Omega_r \Omega_m}{3} \quad (21)$$

$$\frac{d\Omega_r}{dN} = 3\Omega_r[(1+w_\Lambda)\Omega_\Lambda + \Omega_m + \frac{4}{3}\Omega_r] - 4\Omega_r + \frac{\alpha_r \Omega_m (\Omega_\Lambda - \Omega_r)}{3}. \quad (22)$$

Point	Ω_Λ	Ω_m	Ω_r	condition	Eigenvalues
A_1	0	0	0	$w_\Lambda > -1$	$\lambda_1 = -3w_\Lambda - 3$
B_1	0	0	1	$w_\Lambda > 3$, $a > 9$	$\lambda_1 = 9 - 3w_\Lambda$, $\lambda_2 = 9 - a$
C_1	0	1	0	$w_\Lambda > \frac{1}{9}a$, $a < 3$	λ_1= -$3w_\Lambda + \frac{1}{3}a$, $\lambda_2 = -1 + \frac{1}{3}a$
D_1	1	0	0	$w_\Lambda < -1$	$\lambda_1 = 3 + 3w_\Lambda$, $\lambda_2 = 3w_\Lambda - 1$, $\lambda_3 = 3w_\Lambda$

Table 1: The stability, critical points and their eigenvalues of GR corresponding to model I of interaction.

Four critical points were found for the first model of interaction at GR. These critical points are conditionally stable. Point A_1 is stable if $w_\Lambda < -1$, whereas B_1 is stable, if $w_\Lambda > 3$ and $a > 9$. For point C_1, it is stable if $w_\Lambda > \frac{1}{9}a$, $a < 3$. Then, D_1 will be stable when $w_\Lambda < -1$.

- Model II of interaction

The system of equations

$$\frac{d\Omega_\Lambda}{dN} = 3\Omega_\Lambda[(1+w_\Lambda)\Omega_\Lambda + \Omega_m + \frac{4}{3}\Omega_r] - 3(1+w_\Lambda)\Omega_\Lambda + \frac{\alpha_\Lambda \Omega_r (\Omega_\Lambda - \Omega_m)}{3} \quad (23)$$

$$\frac{d\Omega_m}{dN} = 3\Omega_m[(1+w_\Lambda)\Omega_\Lambda + \Omega_m + \frac{4}{3}\Omega_r] - 3\Omega_m + \frac{\alpha_m \Omega_m (\Omega_\Lambda - \Omega_r)}{3} \quad (24)$$

$$\frac{d\Omega_r}{dN} = 3\Omega_r[(1+w_\Lambda)\Omega_\Lambda + \Omega_m + \frac{4}{3}\Omega_r] - 4\Omega_r + \frac{\alpha_r \Omega_\Lambda (\Omega_m - \Omega_r)}{3}. \quad (25)$$

Point	Ω_Λ	Ω_m	Ω_r	w_Λ	Eigenvalues
A_2	0	0	0	$w_\Lambda > -1$	$\lambda_1 = -3w_\Lambda - 3, \lambda_2 = -3, \lambda_3 = -4$
B_2	0	0	1	$w_\Lambda > (\frac{1}{3} + \frac{1}{9}a)$, $a < -6$	$\lambda_1 = 1 - 3w_\Lambda + \frac{1}{3}a$, $\lambda_2 = 1 + \frac{1}{6}a, \lambda_3 = 4$
C_2	1	0	0	$w_\Lambda < (\frac{1}{3} + \frac{1}{9}a)$, $a \leq -12$	λ_1= $3w_\Lambda + 3, \lambda_2 = 3w_\Lambda - 1 - \frac{a}{3}, \lambda_3 = 3w_\Lambda - \frac{a}{6}$

Table 2: The stability, critical points and their eigenvalues of GR corresponding to model II of interaction.

Table 2 shows the critical points gained from applying the second model of interaction on GR. We have point A_2 is stable if it satisfies the condition $w_\Lambda > -1$, while point B_2 is not stable since we have $\lambda_3 = 4$. The last point, C_2, is stable under the conditions $w_\Lambda < (\frac{1}{3} + \frac{1}{9}a)$ and a ≤ -12.

3.2. Teleparallel Equivalence of General Relativity

3.2.1. Cosmological Model

Now, we investigate the cosmological dynamics for the model based on TEGR. The torsion scalor is:

$$T = 6H^2. \tag{26}$$

Then, Friedman equations are:

$$\begin{aligned} 3H^2 &= \kappa^2(\rho + \rho_T) \\ 2\dot{H} &= -\kappa^2[(\rho + P) + (\rho_T + P_T)] \end{aligned} \tag{27}$$

where P_T and ρ_T are the pressure and density of the torsion field. Therefore, beside equation (9) we will have the continuity equation of the torsion field:

$$\dot{\rho}_T + 3H(\rho_T + P_r) = 0 \tag{28}$$

3.2.2. Dynamical Systems and Stability Analysis

- Model I of interaction

For TEGR, the system of density parameter equations corresponding to the first model of interaction (model I):

$$\frac{d\Omega_\Lambda}{dN} = 3\Omega_\Lambda[(1+w_\Lambda)\Omega_\Lambda + \Omega_m + \frac{4}{3}\Omega_r] - 3(1+w_\Lambda)\Omega_\Lambda + \frac{\alpha_\Lambda \Omega_\Lambda \Omega_m}{3} \tag{29}$$

$$\frac{d\Omega_m}{dN} = 3\Omega_m[(1+w_\Lambda)\Omega_\Lambda + \Omega_m + \frac{4}{3}\Omega_r] - 3\Omega_m + \frac{\alpha_m \Omega_r \Omega_m}{3} \tag{30}$$

$$\frac{d\Omega_r}{dN} = 3\Omega_r[(1+w_\Lambda)\Omega_\Lambda + \Omega_m + \frac{4}{3}\Omega_r] - 4\Omega_r + \frac{\alpha_r \Omega_m(\Omega_\Lambda - \Omega_r)}{3} \tag{31}$$

$$\frac{d\Omega_T}{dN} = 3\Omega_T[(1+w_\Lambda)\Omega_\Lambda + \Omega_m + \frac{4}{3}\Omega_r]. \tag{32}$$

The table below (Table 3) shows the critical points of TEGR. It was observed that all critical points are stable under some conditions. Notice that conditions that are not match the fact that w_Λ ranges from $-\frac{1}{3}$ to -1 cannot be met. The interaction parameter a is selected to be in order of unity.

Point	Ω_Λ	Ω_m	Ω_r	Ω_T	w_Λ	Eigenvalues
A_1	0	0	0	0	$w_\Lambda > -1$	$\lambda_1 = -3 - 3w_\Lambda, \lambda_2 = -3, \lambda_3 = -4$
B_1	0	0	0	1	$w_\Lambda > -1$	$\lambda_1 = -3 - 3w_\Lambda, \lambda_2 = -3, \lambda_3 = -4$
C_1	0	0	1	0	$w_\Lambda > \frac{1}{3}$, $a > 3$	λ_1=4, $\lambda_2 = 1 - 3w_\Lambda$, $\lambda_3 = 1 - (\frac{1}{3})a$
D_1	0	1	0	0	$w_\Lambda > \frac{a}{9}$	$\lambda_1 = 3, \lambda_2 = \frac{a}{3} - 1, \lambda_3 = -3w_\Lambda + \frac{a}{3}$
E_1	1	0	0	0	$w_\Lambda < -1$	$\lambda_1 = 3 + 3w_\Lambda, \lambda_2 = 3w_\Lambda - 1, \lambda_3 = 3w_\Lambda$

Table 3: The stability, critical points and their eigenvalues of TEGR corresponding to model I of interaction.

- Model II of interaction

For the second model of interaction, the equations of density parameters are

$$\frac{d\Omega_\Lambda}{dN} = 3\Omega_\Lambda[(1+w_\Lambda)\Omega_\Lambda + \Omega_m + \frac{4}{3}\Omega_r] - 3(1+w_\Lambda)\Omega_\Lambda + \frac{\alpha_\Lambda\Omega_r(\Omega_\Lambda - \Omega_m)}{3} \quad (33)$$

$$\frac{d\Omega_m}{dN} = 3\Omega_m[(1+w_\Lambda)\Omega_\Lambda + \Omega_m + \frac{4}{3}\Omega_r] - 3\Omega_m + \frac{\alpha_m\Omega_m(\Omega_\Lambda - \Omega_r)}{3} \quad (34)$$

$$\frac{d\Omega_r}{dN} = 3\Omega_r[(1+w_\Lambda)\Omega_\Lambda + \Omega_m + \frac{4}{3}\Omega_r] - 4\Omega_r + \frac{\alpha_r\Omega_\Lambda(\Omega_m - \Omega_r)}{3} \quad (35)$$

$$\frac{d\Omega_T}{dN} = 3\Omega_T[(1+w_\Lambda)\Omega_\Lambda + \Omega_m + \frac{4}{3}\Omega_r]. \quad (36)$$

Point	Ω_Λ	Ω_m	Ω_r	Ω_T	w_Λ	Eigenvalues
A_2	0	0	0	0	$w_\Lambda > -1$	$\lambda_1 = -3 - 3w_\Lambda, \lambda_2 = -3, \lambda_3 = -4$
B_2	0	0	1	0	$w_\Lambda > \frac{1}{3} - \frac{a}{18}, a < -6$	λ_1=1-3$w_\Lambda - \frac{a}{6}$, $\lambda_2 = 1 + \frac{a}{6}$, λ_3=4
C_2	1	0	0	0	$w_\Lambda < \frac{1}{3} + \frac{a}{9}$ for $a \leq -12$,$w_\Lambda < -1$ for $a > -12$	$\lambda_1 = 3 + 3w_\Lambda, \lambda_2 = 3w_\Lambda - 1 - \frac{a}{3}, \lambda_3 = 3w_\Lambda - \frac{a}{6}$

Table 4: The stability, critical points and their eigenvalues of TEGR corresponding to model II of interaction.

Similarly, for TEGR the stability of the model is examined and the four fixed points were obtained. The first point, is stable provided that $w_\Lambda > -1$. It is clear that the second point B_2 is unstable because it has a positive eigenvalue $\lambda_3 = 4$. For C_2, it is also conditionally stable, as it is stable, if the following conditions are satisfied:

$$w_\Lambda < \frac{1}{3} + \frac{a}{9} \text{ for a} \leq -12$$
$$w_\Lambda < -1 \text{ for } a > -12$$

and the equation of state reads

$$w_{eff} = \frac{P_{tot}}{\rho_{tot}} = \frac{w_\Lambda\Omega_\Lambda + \frac{1}{3}\Omega_r - \Omega_T}{\Omega_\Lambda + \Omega_r + \Omega_m + \Omega_T} = \frac{w_\Lambda\Omega_\Lambda + \frac{1}{3}\Omega_r - \Omega_T}{1 + \Omega_T}. \quad (37)$$

3.3. Coincidence General Relativity

3.3.1. Cosmological Model

We choose $f(Q)$ expression to be

$$f(Q) = Q + C_1\sqrt{Q} + C_2 \quad (38)$$

where C_1, C_2 are constants and Q is the non-metricity scalar such that $Q = 6H^2$. Referring to equation 7, we will write:

$$3H^2 = \kappa^2(\rho + \rho_Q) \quad (39)$$
$$2\dot{H} = 3H^2 - \kappa^2(P + P_Q). \quad (40)$$

In the above equations, we point out that $\rho = \rho_m + \rho_r$ and $P = P_m + P_r$ as we consider that dark energy part is equal to the non-metricity field $\rho_Q = \rho_\Lambda$, and $P_Q = P_\Lambda$, so

$$\rho_Q = -\frac{C^2}{2\kappa^2}, \quad (41)$$

where $C^2 = -6H^2\Omega_Q$. Therefore the pressure is :

$$P_Q = \frac{C^2}{2\kappa^2}. \quad (42)$$

3.4. Dynamical Systems and Stability Analysis

- Model I of interaction

The system of differential equation for the second model of interaction are:

$$\frac{d\Omega_\Lambda}{dN} = 3\Omega_\Lambda[1-\Omega_\Lambda+\frac{1}{3}\Omega_r] - 3(1+w_\Lambda)\Omega_\Lambda + \frac{\alpha_\Lambda(\Omega_\Lambda\Omega_m)}{3} \tag{43}$$

$$\frac{d\Omega_m}{dN} = 3\Omega_m[1-\Omega_\Lambda+\frac{1}{3}\Omega_r] - 3\Omega_m + \frac{\alpha_m\Omega_m\Omega_r}{3} \tag{44}$$

$$\frac{d\Omega_r}{dN} = 3\Omega_r[1-\Omega_\Lambda+\frac{1}{3}\Omega_r] - 4\Omega_r + \frac{\alpha_r\Omega_m(\Omega_\Lambda-\Omega_r)}{3}. \tag{45}$$

In the same manner, three fixed points were found at CGR (Table 5) and again all points should satisfy a given condition to met the stability.

Point	Ω_Λ	Ω_m	Ω_r	Conditions	Eigenvalues
A_1	0	0	0	$w_\Lambda > 0$	$\lambda_1 = 3w_\Lambda$
B_1	0	0	1	$w_\Lambda < \frac{1}{3}$ for $a > 3$	$\lambda_1 = 1-3w_\Lambda$, $\lambda_2 = 1-\frac{1}{3}a$
C_1	1	0	0	$\frac{-1}{3} < w_\Lambda < 0$	λ_1= -3$w_\Lambda + \frac{1}{3}$ a, $\lambda_2 = -1+\frac{1}{3}a$

Table 5: The stability, critical points and their eigenvalues of CGR corresponding to model I of interaction.

- Model II of interaction

$$\frac{d\Omega_\Lambda}{dN} = 3\Omega_\Lambda[1-\Omega_\Lambda+\frac{1}{3}\Omega_r] - 3(1+w_\Lambda)\Omega_\Lambda + \frac{\alpha_\Lambda\Omega_r(\Omega_\Lambda-\Omega_m)}{3} \tag{46}$$

$$\frac{d\Omega_m}{dN} = 3\Omega_m[1-\Omega_\Lambda+\frac{1}{3}\Omega_r] - 3\Omega_m + \frac{\alpha_m\Omega_m(\Omega_\Lambda-\Omega_r)}{3} \tag{47}$$

$$\frac{d\Omega_r}{dN} = 3\Omega_r[1-\Omega_\Lambda+\frac{1}{3}\Omega_r] - 4\Omega_r + \frac{\alpha_r\Omega_\Lambda(\Omega_m-\Omega_r)}{3}. \tag{48}$$

In Table (6) the stability is tested around four points. First, A_2 is stable when $w_\Lambda > 0$. Second, B_2 is stable if $w_\Lambda > \frac{1}{3}+\frac{1}{9}a$ for $a < -3$.

Point	Ω_Λ	Ω_m	Ω_r	w_Λ	Eigenvalues
A_2	0	0	0	$w_\Lambda > 0$	$\lambda_1 = -3w_\Lambda$, $\lambda_2 = -1$, $\lambda_3 = 0$
B_2	0	0	1	$w_\Lambda > \frac{1}{3}+\frac{1}{9}a$ for $a < -3$	$\lambda_1 = 1-3w_\Lambda+\frac{a}{3}$, $\lambda_2 = 1+\frac{a}{3}$
C_2	1	0	0	$0 < w_\Lambda < \frac{-1}{a-3}$	λ_1= -3$w_\Lambda - \frac{1}{3}w_\Lambda a$, $\lambda_2 = -aw_\Lambda$+3 w_Λ -1, λ_3=-9 w_Λ

Table 6: The stability, critical points and their eigenvalues of CGR corresponding to model II of interaction.

and the equation of state is

$$w_{eff} = \frac{P_{tot}}{\rho_{tot}} = \frac{w_Q\Omega_Q + \frac{1}{3}\Omega_r}{\Omega_Q+\Omega_r+\Omega_m}. \tag{49}$$

4. Results and Discussion

In this section we elaborate the obtained results in plots for different paradigms and different model in each of them. We compare the results between each other and interpret the ability of each model to explain the cosmos.

4.1. Numerical Solutions and Evolutionary Plots

4.1.1. Model-I of interaction

The figures below (Fig. 1), obtained as three-dimensional plots from numerical solutions of dynamical system of the density parameter, show how Ω of the considered fluids are related to each other in model I.

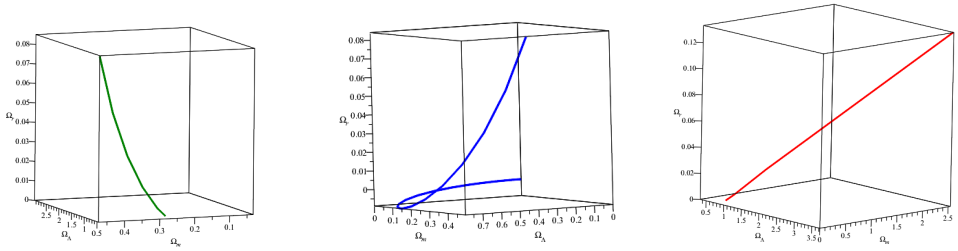

Figure 1. Model I: Density parameters of dark energy, matter and radiation for GR, TEGR and CGR.

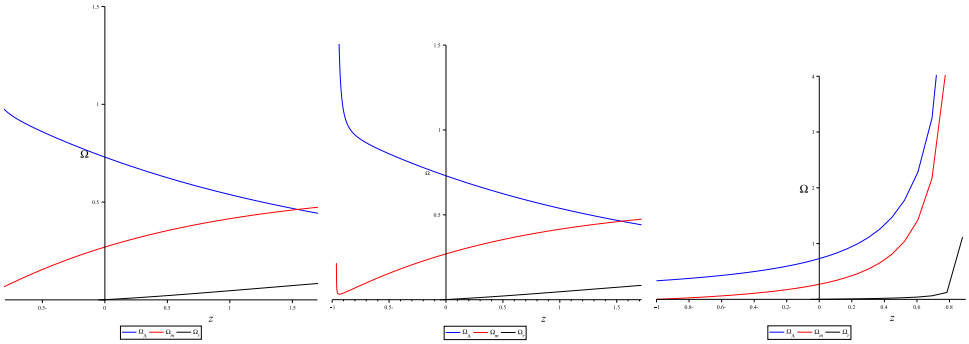

Figure 2. Model I: Numerical solution for the system of density function versus redshift z for GR, TEGR and CGR.

In Fig.2, it was observed that the densities in GR (left) and TEGR (middle) demonstrate nearly similar behavior. There is a point in both figures where dark energy and dark matter acquired the same density in the early time. This is observed at $z \equiv 1.53$ and it indicates an equilibrium point. After this point, the dark energy keeps increasing in later times, while dark matter started to decrease. The density of radiation evolved in the past, However it decreases at $z \equiv -0.05$ and vanishes in the future. On the other hand, for Coincidence General Relativity (right), all of the three ingredients (dark energy, matter and radiation) decrease rapidly with time.

To easily raise a comparison between the three theories, the following plots show each fluid density in separately.

It is noticed in Fig. 3 that densities (Ω_Λ, Ω_m, Ω_r) described by GR (left) and TEGR (middle) exhibit the same behavior, whereas fluids described by CGR (right) shows different behavior. For all fluids, all three paradigms match at $z = 0$ which represents the present time.

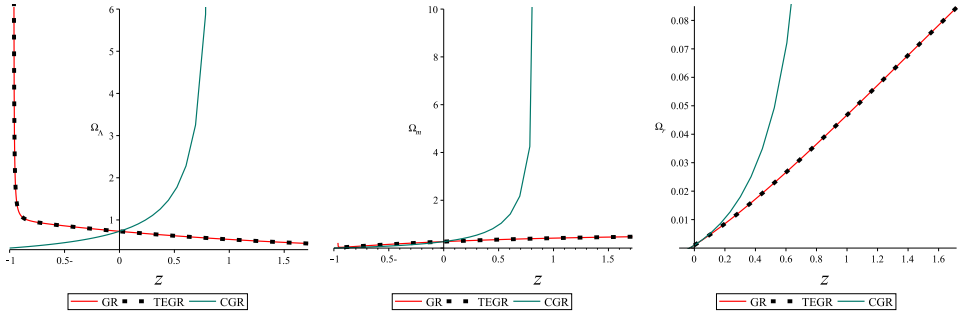

Figure 3. Model I: Dark energy, matter and radiation densities versus redshift z for GR, TEGR and CGR

4.1.2. Model-II

Here, numerical solutions of density parameters were obtained to describe the behavior of fluids under the consideration of the second model of interaction.
Figures 4, represent three-dimensional plots of Ω_λ versus Ω_m versus Ω_r for GR, TEGR and CGR respectively from left to right.

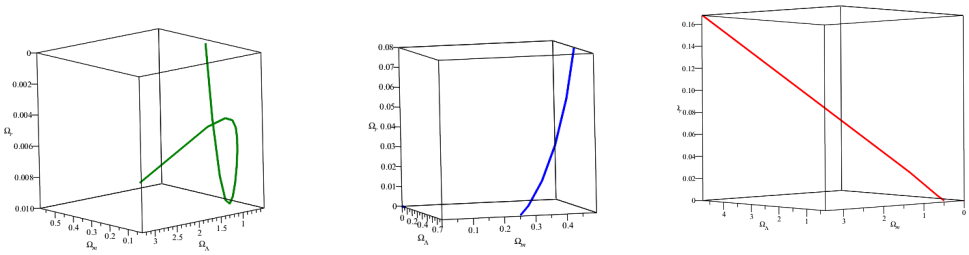

Figure 4. Model II: Density parameters of dark energy, matter and radiation for GR, TEGR and CGR.

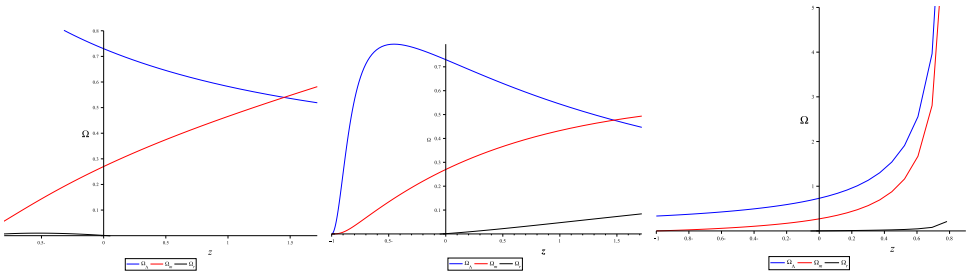

Figure 5. Model II: Numerical solution for the system of density function versus redshift z for GR, TEGR and CGR.

Similarly, numerical solutions for density parameter equations were provided for the three theories corresponding to the dark energy dark matter and radiation. In the first graph in figure 5, we notice that the behavior of the three components in GR do not differ much from model-I of interaction. That is, the dark matter is very large in the early Universe but it may decrease in the future, while dark matter behaves apposite to dark energy. The radiation showed up in the early time epoch with very small amount then fades away. It is worth noting that observations revealed that radiation must exist in the early Universe. Therefore, model-II of interaction is not compatible with the description of GR. For TEGR (the middle graph in figure 5), the dark energy oscillates over time, it arises from very low values, then increased up to $\Omega_\Lambda \approx 0.8$, then it decreased again. Radiation and dark matter increased. According to this model

the early universe consists of dark energy and dark matter as the radiation component emerged later. However, in CGR dark energy and dark matter exponentially decrease with time.

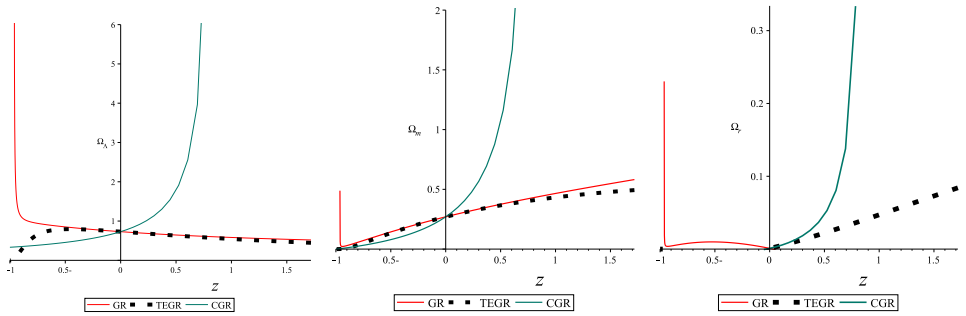

Figure 6. Model II: Dark energy, matter and radiation densities versus redshift z for GR, TEGR and CGR

The combined plots for the Model-II of interaction are shown in figures 6. It is worth mentioning that in the later times of the Universe, each theory has different evolutionary descriptions. The reason is that it is difficult to provide a reliable explanation for the behavior of the fluids in the future. However, we again notice compatible results from GR and TEGR. In figure 6, GR and TEGR show a decrease in dark energy in the early times, while CGR shows an exponential increase. Similarly, for dark matter we can see that the lines of GR and TEGR suitably are paired together up to $z \approx 1$ and go separately beyond this value. Finally, the radiation component is different in each of the three theories.

4.2. Equation of State (EoS)

The left-side graph in figure 7 shows the evolution of the total effective EoS for all the considered fluids (dark energy, dark matter and radiation) described by GR corresponding to the Model-I and Model-II of interaction. We observe that for Model-I the EoS moves from $w_{eff} = -0.04$ to quintessence state ($w_{eff} < -0.3$). However, evolution dedicated by the Model-II, w_{eff} started to evolve from ≈ -0.2 then tends to reach the quintessence state. The lines for both models did not cross $w_{eff} = -1$.

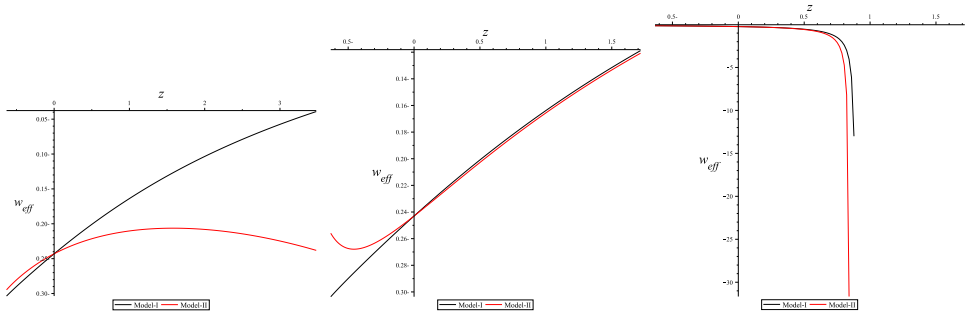

Figure 7. Effective Equation of State w_{eff} versus redshift z for GR, TEGR and CGR

The middle figure, represents the EoS devoted by TEGR. At later times ($z < -0.1$), w_{eff} for both model-I and Model-II, EoS evolves from $w_{eff} \approx -0.1$. Then, at later times EoS for Model-I moves to quintessence while for Model-II it does not reach the quintessence.

Lastly, the Figure in the right-side represents the EoS as described by CGR. The EoS initially started to evolve from phantom state. After that, it continues to cross $w_{eff} = -1$ which is the cosmological constant state.

5. Conclusions and future work

This work investigates the evolution of the Universe demonstrated by GR, TEGR and CGR. Three main types of fluid were presumed of which the Universe constitutes. These fluids are Dark Energy, Dark Matter and Radiation. We propose two models of interaction to express the way the fluids interact with each other.
From the evolutionary plots obtained from numerical solutions, it was found that describing the Universes by curvature in GR and torsion in TEGR lead almost to the same results. However, the non-metricity attributed to CGR gives a distinct explanation. The future of the Universe is difficult to predict as the interaction between the fluids is more complicated than our current knowledge, so it requires a more precise model to demonstrate their interactions. Also, the Equations of State (EoS) were studied as it carries information about the acceleration of the Universe. It was observed that EoS for GR and TEGR behaves like quintessence. However, for CGR the EoS behaves like phantom and it cross the phantom state at $w_{eff} = -1$.
In the subsequent projects one can study the relation of the observational data with respect to the theory of each of these paradigms and the corresponding models. One can tune the parameters used her according to the data with their errors. Some paradigms and models can fit with certain era of the Universe. This can be left to the future to study.

References

1. Jiménez, J. B. Cosmology in f (Q) geometry. *Phys. Rev.* **2020**, *10*,
2. Heisenberg, L. A systematic approach to generalisations of General Relativity and their cosmological implications. *Phys. Rep.* **2019**, *796*, 1-113.
3. Jamil, M. Phase space analysis of interacting dark energy in f (T) cosmology. *Open Phys.* **2012**, *5*, 1065-1071.
4. Jamil, M. Stability of a non-minimally conformally coupled scalar field in F (T) cosmology. *EPJ C* **2012**. *72*, 2075. doi.org/10.1140/epjc/s10052-012-2075-1
5. Lu, J. Cosmology in symmetric teleparallel gravity and its dynamical system. *EPJ C* **2019**, *10*, 530. doi.org/10.1140/epjc/s10052-019-7038-3
6. Jamil, M. Attractor solutions in f (T) cosmology. *EPJ C* **2012**, *10*, 1959. doi.org/10.1140/epjc/s10052-012-1959-4
7. Bamba, K. Phase space description of nonlocal teleparallel gravity. *EPJ C* **2018**, *9*, 771. doi.org/10.1140/epjc/s10052-018-6240-z
8. Bahamonde, S. Modified teleparallel theories of gravity. *Phys. Rev. D.* **2015**, *10*, 104042. doi.org/10.1103/PhysRevD.92.104042
9. Steinhardt, P. J. A quintessential introduction to dark energy. *Journal Abbreviation* **2003**, *10*, 2497-2513.
10. Cai, Y. F. Quintom cosmology: theoretical implications and observations. *Phys. Rep.* **2008**, *1*, 1-60.
11. Boehmer, C. Jacobi stability analysis of dynamical systems—applications in gravitation and cosmology. *Adv. Theor. Math.* **2012**, *4*, 1145-1196.

Author Contributions: Karima Alhosni performed the analytic calculations and performed the the computations.Mudhahir AlAjmi verified the analytical methods and supervised the findings of this work. All authors discussed the results and contributed to the final manuscript

Funding: This research received no external funding

Institutional Review Board Statement: "Not applicable"

Informed Consent Statement: "Not applicable".

Conflicts of Interest: "The authors declare no conflict of interest with any person in any organisation."

Abbreviations

The following abbreviations are used in this manuscript:

MDPI	Multidisciplinary Digital Publishing Institute
DOAJ	Directory of open access journals
TLA	Three letter acronym
LD	Linear dichroism